4452–4462 *Nucleic Acids Research, 2017, Vol. 45, No. 8* *Published online 24 January 2017*
doi: 10.1093/nar/gkx039

Interaction with ZMYND11 mediates opposing roles of Ras-responsive transcription factors ETS1 and ETS2

Joshua P. Plotnik[1] and Peter C. Hollenhorst[2,*]

[1]Biology Department, Indiana University, Bloomington, IN 47405, USA and [2]Medical Sciences, Indiana University School of Medicine, Bloomington, IN 47405, USA

Received September 14, 2016; Revised January 11, 2017; Editorial Decision January 14, 2017; Accepted January 22, 2017

ABSTRACT

Aberrant activation of RAS/MAPK signaling is a driver of over one third of all human carcinomas. The homologous transcription factors ETS1 and ETS2 mediate activation of gene expression programs downstream of RAS/MAPK signaling. ETS1 is important for oncogenesis in many tumor types. However, ETS2 can act as an oncogene in some cellular backgrounds, and as a tumor suppressor in others, and the molecular mechanism responsible for this cell-type specific function remains unknown. Here, we show that ETS1 and ETS2 can regulate a cell migration gene expression program in opposite directions, and provide the first comparison of the ETS1 and ETS2 cistromes. This genomic data and an ETS1 deletion line reveal that the opposite function of ETS2 is a result of binding site competition and transcriptional attenuation due to weaker transcriptional activation by ETS2 compared to ETS1. This weaker activation was mapped to the ETS2 N-terminus and a specific interaction with the co-repressor ZMYND11 (BS69). Furthermore, ZMYND11 expression levels in patient tumors correlated with oncogenic versus tumor suppressive roles of ETS2. Therefore, these data indicate a novel and specific mechanism allowing ETS2 to switch between oncogenic and tumor suppressive functions in a cell-type specific manner.

INTRODUCTION

Mutations activating the RAS/RAF/MEK/ERK (RAS/MAPK) signaling pathway are among the most common drivers of carcinogenesis (1). Activation of this pathway leads to phosphorylation and activation of ERK, which can translocate into the nucleus and phosphorylate a variety of transcription factors leading to altered gene expression (2). These ERK-induced gene expression changes promote oncogenic phenotypes such as increased proliferation, resistance to apoptosis and increased cell migration and invasion (3). Therefore, the transcription factors that mediate the function of the RAS/MAPK pathway represent an important class of therapeutic targets.

The homologous transcription factors, ETS1 and ETS2, are critical nuclear effectors of the RAS/MAPK cascade (4–6). These two proteins are ubiquitously expressed, however relative levels can vary substantially between cell types (7). ETS1 and ETS2 and share 55% amino acid similarity (8). ETS1 and ETS2 both have an ETS DNA binding domain, pointed domain, and ERK and CAMKII phosphorylation sites (9,10). The pointed domain facilitates interactions between ETS1 or ETS2 and the co-activator CBP/p300. Phosphorylation of a threonine neighboring the pointed domain (ETS1 T38/ETS2 T72) by ERK increases affinity of ETS1 and ETS2 for CBP/p300, leading to increased activation of RAS/MAPK target genes (11).

Genetic and biochemical studies demonstrate many functional redundancies between ETS1 and ETS2 during early development, cell survival, cell proliferation and oncogenesis (12,13). ETS1 and ETS2 have identical consensus *in vitro* DNA sequence preferences (14). Mice with a homozygous knockout of ETS1 are viable in some genetic backgrounds (15,16), as are mice where the wild-type (WT) version of ETS2 has been replaced with the phospho-null ETS2 T72A mutation (17). However, homozygous loss of ETS1 in mice coupled with a homozygous ETS2 T72A mutation results in lethality, indicating a redundant function that requires ERK phosphorylation (12). In Head and Neck Squamous Cell Carcinoma (HNSCC), ETS1 and ETS2 both function as drivers of oncogenesis. Elevated expression of both factors is observed in HNSCC tumors compared to normal mucosa and this results in increased expression of oncogenes such as *CIP2A* (18), *CXCL1/2* (19) and *Vimentin* (20). Likewise, expression levels of both ETS1 and ETS2 correlate with higher histological grading and poorer outcomes of ovarian and endometrial cancers (21,22).

Despite evidence of redundant functions in many systems, there are reports of ETS1 and ETS2 having opposite functions. One example is the ability for ETS1 to repress B-cell differentiation through activation of the *BLIMP1* gene, while ETS2 cannot activate *BLIMP1* expression (23). In tu-

*To whom correspondence should be addressed. Tel: +1 812 855 1151; Fax: +1 812 855 4436; Email: pchollen@indiana.edu

mors, ETS1 appears to function consistently as an oncogene (24), however ETS2 is often reported to be a tumor suppressor (25). An extra copy of ETS2 present in mice harboring Trisomy XXI conferred resistance to the formation of solid tumors driven by APC(Min) (26). In non-small cell lung cancers, ETS2 expression functions to inhibit expression of the *MET* oncogene and weakens RAS/MAPK signaling intensity (27). Recently, it has been shown that the loss of one copy of ETS2 that occurs during TMPRSS2-ERG gene rearrangements in prostate cancer leads to more aggressive prostate tumors and poor survival outcome (28). We recently described a critical role for ETS1 as an effector of RAS/MAPK signaling in cancer cell lines containing mutant KRAS, however, we found that ETS2 has the opposite function (6). Taken together, these findings indicate an oncogenic role for ETS1, but a role for ETS2 that can be either oncogenic or tumor suppressive depending on the cellular background. However, the molecular mechanisms that allow ETS2 to function as a tumor suppressor are unknown.

Here, we report that ETS1 and ETS2 divergently regulate a common cell migration gene expression program in prostate cancer cells. Mapping the ETS2 cistrome showed that it binds to the same regions as ETS1. These regions have ETS/AP1 binding sequences and occur near genes involved in cell migration. ETS2 reduced gene expression in the presence of ETS1, but activated in the absence of ETS1 supporting a competition model where ETS2 acts as a weaker activator than ETS1. Using a panel of chimeric ETS1/2 constructs we demonstrate that the N-terminal region of ETS2 reduces activation compared to ETS1, and this region specifically interacts with the co-repressor ZMYND11. Binding of ZMYND11 to ETS1/2 co-bound regions increased in the ETS1 knockout, consistent with binding site competition. Knockdown of ZMYND11 in the ETS1 knockout rescued the cell migration phenotype indicating that this molecule is key to attenuation by ETS2. High expression of ZMYND11 predicted improved recurrence free survival in patients with prostate cancer. Finally, high ZMYND11 expression levels in tumors correlate with a tumor suppressive function of ETS2 across many epithelial tumors. Together, these data indicate that the ZMYND11 interaction is a specific mechanism for the cell type dependent tumor suppressive function of ETS2.

MATERIALS AND METHODS

Cell culture and viral transduction

Cell lines were cultured by ATCC recommendation as follows: EBNA293, HEK-293T, DU145 were grown in Dulbecco's modification Eagle (DMEM) [Sigma] with 10% fetal bovine serum (FBS) [Sigma]. A549 cells were grown in F12K (Sigma) with 10% FBS [Sigma]. All media included 1× Penicillin/Streptomycin (Mediatech-Cellgro).

Lentivirus for ETS factor shRNA was produced by co-transfection of pLKO.1 (Addgene plasmid 8453) (29) with shRNA sequences (Supplementary Table S1) in HEK293T cells with pMDLg/pRRE (Addgene plasmid 12251), pRSV-Rev (Addgene plasmid 12253) and pMD2.G (Addgene plasmid 12259) packaging plasmids (30) as previously described (31).

RNA sequencing and analysis

Total RNA for three independent biological replicates was isolated from DU145 cells transduced with lentiviral shRNA knockdown vectors (see above) using the RNeasy mini kit (Qiagen) according to manufacturer's instructions. Sequencing libraries for whole transcriptome analysis were generated by Illumina TruSeq sample preparation protocol. Number of mapped reads as determined by Samtools from TopHat output is found in Supplementary Table S2 and clustering of RNA-seq replicates can be found in Supplementary Figure S1A.

Data files are available for download from NCBI's Gene Expression Omnibus (GEO; http://www.ncbi.nlm.nih.gov/geo/), accession number GSE59020 (ETS1 shRNA) or GSE86240 (ETS2 shRNA).

Generation of ETS1 knockout cell lines

ETS1 knockout lines were generated using the D10A Cas9 Nickase, pX335-U6-Chimeric_BB-CBh-hSpCas9n(D10A) (Zhang, Addgene #42235). Guide RNA's (gRNA) were generated using algorithms found at crispr.mit.edu (Supplementary Table S1). gRNA's were cloned into the Cas9 backbone as described previously (32) and 5 μg of each gRNA was transfected into DU145 cells. Puromycin (5mg/mL) was added at 24 h, and washed out at 48 h. Transfected cells were counted and diluted to a concentration of 1 cell/200 μl. In a 96-well plate, 100 μl of diluted cells were plated and allowed to grow to confluence. Single colonies were tested for knockout via protein immunoblotting (described below). CRISPR/Cas9 generated indels were identified via gDNA PCR and sequencing of individual clones.

Protein immunoblotting and RNA quantification

Total protein extract from equal number of cells were separated on 10% sodium dodecyl sulphate-polyacrylamide gel electrophoresis gels, transferred to nitrocellulose membrane (Bio-Rad), blocked in 5% milk in TBS (10 mM Tris, pH8.0, 150 mM NaCl), incubated with primary and secondary antibodies and visualized by ECL (Thermo Scientific) using standard procedures. Antibodies were the same as for ChIP plus anti-FLAG (Sigma) and anti-Tubulin (Sigma).

RNA levels were measured by reverse transcription followed by quantitative RT-PCR with standard curves as described previously (7) using DNA oligonucleotides in Supplementary Table S1. RNA levels were normalized to 18S rRNA.

Transwell migration assays

Transwell migration assays were carried out as previously described (33), with minor modifications. In brief, 1×10^5 cells were introduced to the transwell (8 μM pore size; BD Bioscience) and incubated 24 h. Cells containing overexpression vectors were transiently transfected using Transit2020 (Mirus) 24 h prior to performing migration assay. Each experiment is three biological replicates containing the mean of two technical replicates.

Chromatin immunoprecipitation and sequencing

ChIP was carried out as previously described (33). In short, cells were crosslinked using 1% v/v Formaldehyde (Fisher Scientific) for 15 min and quenched with 2M Glycine for 5 min. Isolated cells were lysed and sonicated for 3 min (30 s ON/OFF) [Daigenode, Bioruptor Pico]. Nuclear lysate was rotated with speciifc antibody for 4 h at 4°C, washed, and DNA isolated by phenol/chloroform. ChIP antibodies used were from Santa Cruz Biotechnology: the dual specificity ETS1/ETS2 antibody was x-ETS2 (sc-351, lot #H2115), the ETS1 specific antibody was ETS1 (sc-350, lot #F1312) and ZMYND11 (sc-292571, lot #K1814). Library preparation was carried out as previously described (6). Peak calling and downstream analysis including intersect regions used the USeq platform (http://useq.sourceforge.net/). Cross correlation analysis (NSC/RSC values) is in Supplemental Table S3.

ChIP-seq Data files generated in this study can be found via Gene Expression Omnibus (http://www.ncbi.nlm.nih.gov/geo/) accession number GSE86240. Data sets reanalyzed were obtained via accession number GSE59021 (6).

Motif searching and ontology analysis

Enriched motif searching was accomplished using the RSAT 'peak motifs' platform (http://rsat.sb-roscoff.fr/). Settings for motif enrichment using RSAT are as followed: Discover over-represented words and discover words with local over-representation at an oligomer length of 6, 7 and 8. Number of motifs returned per algorithm was set equal to 5. All other options remained as default settings. Ontology searches were done using g:Profiler (http://biit.cs.ut.ee/gprofiler/). Settings for g:Profiler ontology algorithm are as followed: output style—textual, max functional category—1500, significant only. All other settings remained default. Significance is shown as corrected *P*-value.

Pull down and co-immunoprecipitation assays

His-tagged purified ETS (34) were diluted in 300 μl binding/wash buffer (100 mM Sodium phosphate pH 8.0, 600 mM NaCl and 0.02% Tween 20) and incubated with 2.5 μl of His-tag Dynabeads (Life Technologies) for 2 h in a rocker. Unbound ETS proteins were removed by washing the beads two times with binding/wash buffer. With the bead bound ETS proteins, ∼14 μg of PC3 nuclear extracts (sc-2152, Santa Cruz Biotechnology) along with 100 μg of BSA were rotated for 1–2 h. Beads were washed four times with NP-40 lysis buffer and proteins eluted using sodium dodecyl sulphate (SDS) protein loading dye. Eluted proteins were separated in a SDS gel and transferred to a nitrocellulose membrane, which was Ponceau stained (0.1 in 5% acetic acid) and immunoblotted.

For co-immunoprecipitation, whole-cell extracts were isolated from DU145 cells using cell lysis buffer (50 mM Hepes-KOH pH 8.0, 140 mM NaCl, 1 mM EDTA, 0.5 mM EGTA, 10% glycerol, 0.5% Nonidet p40, 0.25% Triton X-100). Indicated antibodies were added to supernatants and rotated overnight in a rocker at 4C. 50 μl of respective Dynabeads (Invitrogen) were then added and rotated for 4 h in a rocker. Beads were washed four times with NP-40 lysis buffer and immunoblotted.

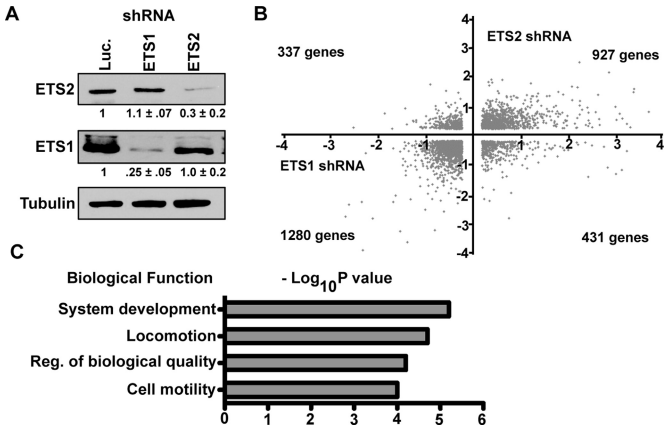

Figure 1. ETS1 and ETS2 divergently regulate a cell migration gene expression program. (**A**) Representative immunoblot of DU145 cells stably expressing ETS1, ETS2, or, as a control, luciferase (luc.) shRNA. Anti-tubulin blot is a loading control. Image J quantification of three independent biological replicates relative to the luciferase shRNA is shown as mean and SEM under each lane. (**B**) Dot plot of differential gene expression from triplicate RNA-sequencing of DU145 cells with control shRNA compared to DU145 with ETS1 or ETS2 shRNA. Only direct ETS1 target genes in DU145 as determined by ChIP-seq (6) are shown. Number in each quadrant indicates the quantity of genes with expression changes of $\log_2 > 0.2$ in both the ETS1 shRNA and ETS2 shRNA clones. (**C**) Gene ontology analysis of 337 genes activated by ETS1 but repressed by ETS2 expression ranked by $-\log_{10}P$-value.

TCGA data curation and Kaplan–Meier curve analysis

RNA-sequencing analysis of patient tumor data curated by the TCGA consortium (35) was analyzed using UCSC Cancer Browser (https://genome-cancer.ucsc.edu). Relevant survival data was downloaded and Kaplan-Meier curve analysis, along with *P*-value generation were analyzed using the 'Survival' library within the R suite as described at the package website (https://cran.r-project.org/web/packages/survival/index.html). For ZMYND11/ZMYND11 expression analysis across tumors, expression data was downloaded from cBioPortal (http://www.cbioportal.org/) and reconstituting using Prism analysis software.

RESULTS

ETS1 and ETS2 divergently regulate a cell migration gene expression program

We previously reported that ETS1 promotes and ETS2 represses migration of DU145 prostate cancer cells (6); however, it remained unclear if this divergent function was due to opposite regulation of a common gene expression program or via unique target genes. To test if ETS1 and ETS2 regulate a common cell migration gene expression program, we carried out differential expression analysis by RNA-sequencing using three biological replicates of DU145 cells with shRNAs targeting ETS1, ETS2 or luciferase control (Figure 1A). To examine direct target genes, we only considered genes with neighboring ETS1 binding sites based on previous ChIP-seq in DU145 cells (6). The majority (74.2%)

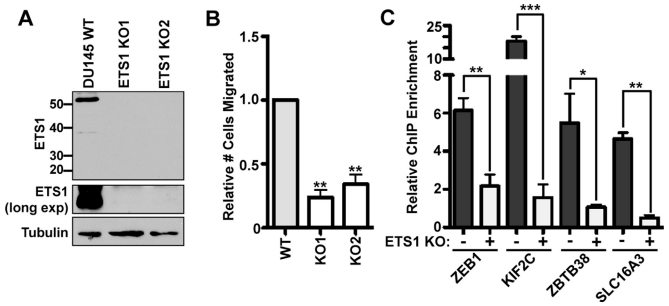

Figure 2. Characterization of a functional CRISPR/Cas9 mediated DU145 ETS1 knockout. (**A**) Immunoblot of two ETS1 knockout (KO) lines compared to DU145 wild-type (WT) parental. Extended region below ETS1 band is shown to indicate that no novel spliced or truncated versions of ETS1 were detected. Size markers in kb on left. Anti-tubulin used as a loading control. (**B**) Transwell migration assay demonstrating ETS1 KO relative to WT as the mean and SEM ($n = 3$). (**C**) Chromatin immunoprecipitation (ChIP) enrichment for ETS1 by qPCR at known ETS1 binding sites compared to an unbound control locus. All *P*-values (* < 0.05, ** < 0.01, *** < 0.001) by *t*-test as compared to WT.

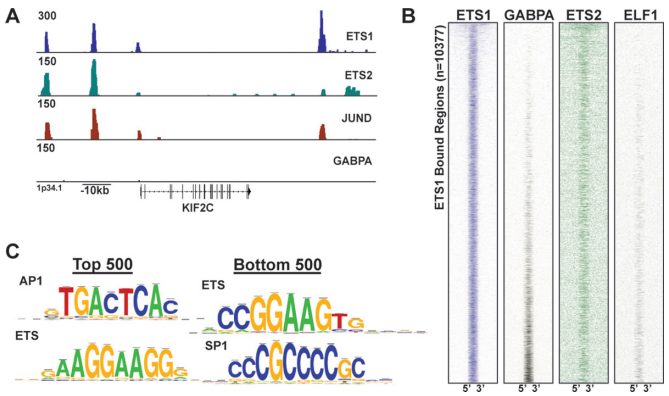

Figure 3. ETS2 binds to the same sites as ETS1 across the genome. (**A**) ETS1, ETS2, JUND and GABPA occupancy near the gene encoding KIF2C is plotted by -log binomial *P*-value from ChIP-seq data in DU145 (ETS1, JUND, GABPA) or DU145 ETS1 KO cells (ETS2) and normalized to DU145 genomic input by USeq (**B**) Heatmap of enrichment of ETS factors at all DU145-ETS1 bound regions ranked by difference between intensities of ETS1 and GABPA. Bound region indicated as 5′ to 3′ with an extended view +/− 7kb in either direction and normalized to DU145 genomic input by NGSPlot. (**C**) First and second most enriched motifs in top 500 or bottom 500 genomic regions shown in (B).

of genes that changed in expression were either activated by both ETS1 and ETS2, or repressed by both ETS1 and ETS2, consistent with a common a role for these two proteins at a large portion of the ETS1 cistrome (Figure 1B and Supplementary Table S4). To investigate why ETS1 and ETS2 have opposite functions in cell migration we focused on 337 genes activated by ETS1 (down in ETS1 shRNA) and repressed by ETS2 (up in ETS2 shRNA). A gene ontology search using g:Profiler indicated that the most enriched functions of these genes included development, locomotion and cell motility (Figure 1C and Supplementary Table S5). These categories were not found significantly enriched in other quadrants (Supplementary Table S5). These data indicate that, consistent with the migration phenotype, ETS1 and ETS2 regulate expression of cell migration genes in opposite directions.

The transcriptional factor ZEB1 was one of the 337 direct target genes activated by ETS1 and repressed by ETS2. ZEB1 is known to repress epithelial gene expression leading to epithelial-mesenchymal transition and increased cell migration (36). Interestingly, an unbiased search for over-represented sequence motifs in ETS1-bound regions near ETS1-repressed genes indicated that ZEB1 binding sites were the most enriched sequence (Supplemental Figure S1B). For repressed genes, the ZEB1 binding sequence was even more enriched than the ETS binding sequence, whereas the ETS sequence was most enriched near ETS1-activated genes. These data indicate that, despite nearby ETS1 binding, that ETS1 mediated repression may occur via the indirect effect of increased ZEB1 expression.

ETS2 and ETS1 bind the same sites genome-wide

One model that could explain both redundant and opposite roles for ETS1 and ETS2 would be if these proteins compete for the same cis-regulatory sequences, but vary in their ability to promote transcription. Therefore, we wanted to test whether ETS2 binds the ETS1 cistrome. While the ETS1 antibody is specific, all ETS2 antibodies tested also recognized ETS1 (Supplementary Figure S1C) making it impossible to verify that an overlapping ChIP signal was coming from ETS2, and not ETS1 in cells that express both. To overcome this technical limitation, we created a CRISPR/CAS9 driven ETS1 knockout in DU145 cells using two guide RNAs in nickase plasmids that target ETS1 exon 3, the first exon present in all ETS1 isoforms (Supplementary Figure S2A). After clonal expansion, knockouts were verified by cloning ETS1 exon 3 into a vector backbone and sequencing to a depth of $n > 5$. Two knockout clones were generated, each with nonsense mutations caused by a common 38 bp duplication in one allele and a unique random insertion of either 10 or 25 bp in the other allele (Supplementary Figure S2B). Loss of ETS1 protein expression confirmed the sequencing results (Figure 2A), and loss of cell migration (Figure 2B) in these strains was consistent with shRNA knockdowns (6). Further, ETS2 expression did not change in the two ETS1 knockout clones (Supplementary Figure S2C). To further verify loss of ETS1, chromatin occupancy was tested at known ETS1 targeted sites via ChIP quantitative PCR in WT and ETS1 knockout DU145 cell lines. We observed a significant reduction in ETS1 ChIP signal at all sites tested in the knockout compared to WT (Figure 2C). Together these data indicate a functional knockout of ETS1 in DU145 and provides a tool to study the specific roles of ETS2 throughout the cistrome.

The DU145 ETS1 knockout cell line was then used with the ETS1/ETS2 dual specificity antibody for ChIP-seq to determine genome-wide ETS2 binding sites. A subset of bound regions were validated by ChIP-qPCR (Supplementary Figure S3A). Of the 1018 ETS2-bound regions identified by peak calling, 581 (57%) overlapped with regions bound by ETS1 in WT DU145 cells (Supplementary Figure S3B). ETS1 and ETS2 had overlapping occupancy at regulatory sites associated with cell migration genes that were in the group of 337 activated by ETS1 and repressed by ETS2, such as *KIF2C, ZBTB38, ZEB1* and *SLC16A3* (Figure 3A and Supplementary Figure S3C–E). We have

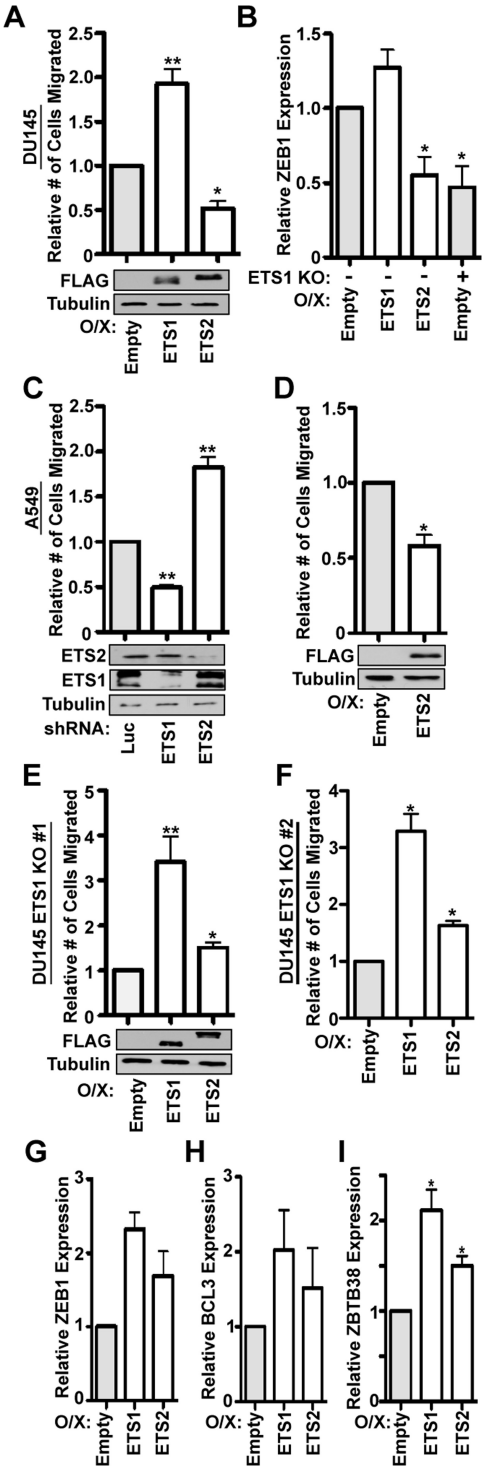

Figure 4. ETS2 functions as a weak activator compared to ETS1. (**A**) Transwell migration of DU145 cells expressing FLAG-ETS1 or FLAG-ETS2 are shown relative to DU145 cells with empty vector as a mean and SEM ($n = 3$). (**B**) ZEB1 mRNA levels measured by RT-qPCR (normalized to 18s rRNA) in DU145 cells expressing FLAG-ETS1 or FLAG-ETS2 or DU145 ETS1 KO cells compared to DU145 cells with empty vector shown as mean and SEM ($n = 3$). (**C**) Transwell migration of A549 lung cancer cells expressing ETS1 or ETS2 shRNA shown relative to A549 luciferase shRNA control as mean and SEM ($n = 3$). (**D**) Transwell migration of A549 lung cancer cells expressing FLAG-ETS2 shown relative to A549 empty control as mean and SEM ($n = 3$). (**E**) Transwell migration of DU145 ETS1 KO cells expressing FLAG-ETS1 or FLAG-ETS2 shown relative to DU145 ETS1 KO empty vector as mean and SEM ($n = 3$). (**F**) As in (E) but in second ETS1 KO clone. (**G**) ZEB1 mRNA levels as in (B), but in DU145 ETS1 KO cells. (**H**) Relative BCL3 or (**I**) ZBTB38 mRNA expression in DU145 ETS1 KO cells as in (G). All *P*-values (* < 0.05, ** < 0.01, *** < 0.001) by *t*-test compared to control.

previously shown that ETS1 can bind to two classes of binding sites; sites bound by many different ETS factors, which tend to be in the proximal promoters of housekeeping genes (redundant sites), and sites bound more specifically by ETS1, which tend to be in distal enhancers of tissue-specific genes (specific sites) (37,38). The ETS/AP-1 sequence elements that regulate expression of cell migration genes tend to be in specific enhancer sites (6), therefore we hypothesized that, like ETS1, ETS2 might bind both redundant and 'ETS1 specific' sites. Because the ETS factor GABPA binds almost exclusively to the redundant, promoter sites, we rank-ordered ETS1-bound regions by GABPA ChIP-seq signal in DU145 cells to separate redundant and specific classes (Figure 3B). ETS2-bound regions overlapped equally with both redundant and specific classes of ETS1 binding sites, indicating overlapping ETS1 and ETS2 binding across the entire ETS1 cistrome. As a control, we also compared DU145 ChIP-seq signal for a fourth ETS factor, ELF1. As expected, ELF1 only overlapped at the redundant (GABPA occupied), but not the specific class of ETS1 sites (Figure 3B). To further characterize regions bound by ETS1 and ETS2, we determined over-represented sequence motifs in the ETS1 and ETS2 ChIP-Seq datasets. The top 500 (Figure 3B) specific ETS1/2 co-bound regions were compared to the bottom 500 redundant ETS bound regions (bound by ETS1, ETS2, GABPA and ELF1) by unbiased motif search. The specific ETS1/2 co-bound regions were most enriched for ETS and AP-1 transcription factor binding sites (Figure 3C). Interestingly, the ETS binding sequence identified is similar to the GGAA repeat sequence bound by EWS-FLI1 in Ewing's sarcoma (39). Conversely, the redundant (bound by all ETS) sites were enriched for a consensus ETS sequence and the SP1 sequence (Figure 3C). JUND, an AP-1 subunit, also had overlapping binding with ETS1 and ETS2 at key regulatory sites (Figure 3A and Supplementary Figure S3C–E). We then asked whether the specific ETS1/2 regions were found proximal or distal to transcriptional start sites (TSS). 79% of specific sites were in distal regulatory elements (>300 bp from TSS), while 78% of redundant ETS sites were located in proximal promoter (<300 bp from TSS) neighborhoods (Supplementary Figure S3F). Ontology search algorithms determined that unique ETS1/2 bound regions were near genes involved in migration functions such as focal adhesion ($P = 5.9 \times 10^{-17}$) and cell-substrate adherens junction ($P = 9.8 \times 10^{-17}$) (Table 1). Together these data indicate that ETS2, like most other ETS factors, can bind the consensus ETS sequences often found in housekeeping gene promoters, but ETS2 can also bind the ETS/AP-1 sites that are ETS1 targets in the enhancers of cell migration genes.

Table 1. Roles of unique (top 500) versus redundant (bottom 500) ETS1/2 co-bound regions

Category	Most over-represented ontologies	*P*-value
Unique, top 500	Focal adhesion	5.9×10^{-17}
	Cell-substrate adherens junction	9.8×10^{-17}
	Translational elongation	3.7×10^{-10}
	Chromatin silencing	1.2×10^{-8}
Redundant, bottom 500		
	RNA processing	7.5×10^{-13}
	tRNA processing	1.7×10^{-8}
	Ribosome biogenesis	2.6×10^{-8}
	rRNA processing	2.8×10^{-4}

ETS2 functions as a weak activator in the absence of ETS1

In DU145 prostate cancer cells ETS1 promotes migration and activation of EMT genes such as *Vimentin*, while ETS2 has the opposite function (6). Consistent with this, when over-expressed, ETS2 significantly reduced DU145 cell migration and reduced expression of the master EMT regulator *ZEB1*, while ETS1 activated both (Figure 4A and B). In fact, ETS2 over-expression reduced ZEB1 expression to a similar extent as the ETS1 knockout (Figure 4B). To test if this function of ETS2 extends to other cancer cell lines, ETS2 was knocked down and over-expressed in A549 non-small cell lung cancer cells and changes in cell migration were measured (Figure 4C and D). Similar to DU145 cells, ETS2 acts as a repressor of cell migration and thus opposite to ETS1 in A549 cells. To reduce expression of cell migration genes, ETS2 could be acting as a transcriptional repressor, or alternatively, ETS2 could simply be a weaker activator than ETS1, resulting in lower expression when it displaces ETS1 at cis-acting sequences. To differentiate between these models, we tested roles of ETS1 and ETS2 in DU145 cells with an ETS1 knockout. In two unique ETS1 knockout CRISPR clones, expression of exogenous ETS1 rescued the ∼3-fold reduction in cell migration that occurred when ETS1 was deleted (Figure 4E and F, compare to Figure 2B). Interestingly, in the ETS1 knockout line, ETS2 also functioned as an activator of cell migration, albeit to a lesser extent than ETS1 (Figure 4E and F). We also tested expression of a subset of the 337 genes activated by ETS1 and repressed by ETS2 in WT DU145 cells (Figure 1B). *ZEB1, BCL3* and *ZBTB38* expression in DU145 ETS1 knockout cells followed the same trend as the migration phenotype, with both ETS1 and ETS2 increasing expression, but ETS1 to a greater extent. (Figure 4G–I). These data suggest a role for ETS2 that is not repression, but attenuation due a weaker transcriptional activator (ETS2) replacing a stronger transcriptional activator (ETS1).

The N-terminal portion of ETS2 is responsible for weaker activation than ETS1

To identify the mechanism behind the weaker function of ETS2 compared to ETS1, we sought to identify the protein domain responsible. We created ETS1/2 chimeric constructs that replaced either the N-terminus, Middle region, or C-terminus of ETS1 with the corresponding region of ETS2 (Figure 5A). These ETS1/2 chimeras were transiently transfected into DU145 prostate cancer cells to similar protein expression levels (Figure 5B). The transfected cells were

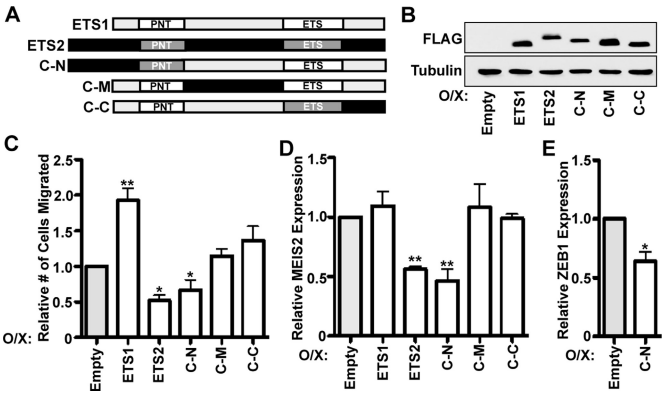

Figure 5. The N-terminal region of ETS2 is sufficient for reduced activation function compared to ETS1. (**A**) A schematic of ETS1 and ETS2 showing the two known structured domains; pointed (PNT) and ETS DNA binding (ETS). Chimeric ETS1/2 constructs are indicated and named C-N, C-M and C-C for chimera of the N-terminus, middle and C-terminus, respectively. Darker shaded regions indicate portions stemming from ETS2, lighter from ETS1. (**B**) Anti-FLAG immunoblot of DU145 whole cell extract expressing FLAG tagged ETS1, ETS2 and chimeric constructs with tubulin as a control. (**C**) Transwell migration of DU145 prostate cancer cells expressing indicated ETS1/2 constructs relative to empty vector, shown as mean and SEM ($n = 3$). (**D**) Relative MEIS2 messenger RNA expression in DU145 cells expressing ETS1/2 constructs normalized to 18S rRNA and relative to empty vector shown as mean and SEM ($n = 3$). (**E**) Relative ZEB1 expression as in (D). All *P*-values (* < 0.05, ** < 0.01) by *t*-test compared to empty vector.

then examined to identify which chimeras acted like ETS2 by decreasing cell migration and expression of target genes such as *ZEB1* and *MEIS2*. Only the chimera consisting of ETS1 with the ETS2 N-terminus significantly decreased cell migration (Figure 5C) and both *MEIS2* and *ZEB1* expression (Figure 5D and E), like ETS2. To further validate the function of the ETS2 N-terminus, we deleted amino acids 1–68 of ETS2 and found that loss of this region abrogated the attenuation function of ETS2 over-expressed in A549 cells (Supplementary Figure S4A). These data indicate that the weaker function of ETS2 compared to ETS1 stems from the ETS2 N-terminus.

ETS2 specifically recruits the co-repressor ZMYND11 to ETS1/2 co-bound regions

We postulated that the difference between the N-terminus of ETS1 and ETS2 is likely a differential interaction with a co-regulator. The transcriptional co-repressor ZMYND11 (BS69) has been reported to interact with the N-terminus of

ETS2 (40), but interaction with ETS1 has not been tested. To compare binding, purified ETS1 and ETS2 were immobilized and used to pull-down proteins from PC3 nuclear extract. A ZMYND11 interaction was assayed by immunoblot. Strikingly, ZMYND11 interacted specifically with ETS2, and not ETS1 (Figure 6A). A specific interaction that depends on the ETS2 N-terminus was further validated by reverse co-immunoprecipitation of ZMYND11 in DU145 cells expressing FLAG-ETS1, FLAG-ETS2, or a FLAG-tagged chimera consisting of ETS1 with the ETS2 N-terminus. Probing the ZMYND11 immunoprecipate with a FLAG antibody showed that ETS2 and the chimeric construct, but not ETS1, interacted with ZMYND11 in cells (Figure 6B). Therefore, the weaker activating function that can be imparted by the ETS2 N-terminus coincides with a specific interaction with ZMYND11.

Based on these findings, we proposed a model where ETS1 and ETS2 compete for the same binding sites, and when ETS2 is bound it recruits ZMYND11, resulting in reduced transcriptional activation. To test this model across the ETS1/ETS2 cistrome we mapped ZMYND11 binding by ChIP-seq in both DU145 and ETS1 knockout DU145 cells. ZMYND11 binding was enriched within gene bodies as previously reported (41), however upon ETS1 deletion, we observed an increase in ZMYND11 occupancy of promoters and proximal enhancers—regions where ETS1 and ETS2 often bind (Supplementary Figure S4B). We then focused directly on the 581 regions bound by ETS1 in DU145 cells and by ETS2 in ETS1 knockout DU145 cells, which we considered sites of potential ETS1/ETS2 competition. At these sites, we observed a dramatic induction of ZMYND11 binding when ETS1 was knocked out (Figure 6C and D). This suggested that ZMYND11 is bound to these regions more often when ETS2 binding increases due to loss ETS1 competition. As a control, we compared binding in regions where ZMYND11 binds independently of ETS1/2 in both cell lines. These regions had similar ZMYND11 enrichment in both lines (Figure 6D, lower panel), indicating that the observed change in ZMYND11 enrichment is specific to ETS1/ETS2 target sites. Using ChIP-qPCR we confirmed that ETS1 knockout cells had a significant increase in ZMYND11 enrichment at known ETS1/2 bound sites near the ZEB1, KIF2C, ZBTB38 and SLC16A3 genes (Figure 6E). Consistent with these findings, 82% of the 581 ETS1/ETS2-bound regions were co-occupied by ZMYND11 in ETS1 knockout cells (Supplementary Figure S3B). Examination of ZMYND11 occupancy at *ZBTB38*, *KIF2C* and *ZEB1* enhancers also revealed co-occurrence with ETS1 and ETS2 binding sites (Figure 6F). Further, we observed that 53% of the ETS1-bound regions near genes activated by ETS1 and repressed by ETS2 were co-occupied by ZMYND11 in the ETS1 knockout line. This was a significantly higher overlap than at regions near genes repressed by ETS1 or activated by ETS2 (28-37%) (Supplementary Figure S4C). This indicates that ZMYND11 binds specifically to ETS1/2 bound regions near cell migration genes activated by ETS1 and repressed by ETS2. These data, taken together, provide evidence of binding site competition between ETS1 and an ETS2/ZMYND11 complex, and a potential explanation for opposite roles of ETS1 and ETS2.

ZMYND11 is necessary for repressive functions of ETS2 and is a tumor suppressor

To test if ZMYND11 is responsible for the opposite role of ETS2 compared to ETS1, an shRNA was used to knockdown ZMYND11 expression in DU145 cells (Figure 7A). Reduced ZMYND11 had little effect on migration of WT DU145 cells (Figure 7B), possibly because ETS1 is bound to the ETS/AP-1 regulatory sequences more often than ETS2. When ETS2 is over-expressed in DU145 cells to tilt the competitive balance toward ETS2, this resulted in less cell migration (Figure 3A). Strikingly, when ZMYND11 levels are reduced, this repressive effect of ETS2 over-expression on cell migration is eliminated (Figure 7B). Consistent with this finding, when we knocked down ZMYND11 in ETS1 knockout DU145 cells, where only ETS2 would be occupying the ETS1/2 specific sites, there was a significant increase in cell migration (Figure 7C). Interestingly, this boost in migration (approximately 3-fold) was similar to the extent that ETS1 rescued migration in the ETS1 knockout (Figure 4E). This data is consistent with the difference between ETS1 and ETS2 stemming from the ETS2/ZMYND11 interaction.

If ZMYND11 is necessary for ETS2 to act like a tumor suppressor, then differences in ZMYND11 expression level could explain cell-type specific roles of ETS2 as a tumor suppressor. To test this, we used TCGA RNA-sequencing data to rank all epithelial tumor types with greater than 75 sequenced tumors from lowest to highest median ZMYND11 expression (Supplementary Figure S5). The ability of ETS2 to act like a tumor suppressor was then assessed in each cancer type by comparing outcomes for patients with tumors where ETS2 expression was higher than ETS1 versus those where ETS1 expression is higher than ETS2. In the five cancers with the lowest ZMYND11 levels, there was no clear benefit to having higher ETS2 than ETS1 (Supplementary Figure S5). However, in the five carcinomas with the highest median ZMYND11 expression there was a trend toward longer recurrence free survival if ETS2 levels were higher than ETS1, and in two of these (non-small cell lung cancer and prostate adenocarcinoma) this trend was statistically significant ($P < 0.05$). This is consistent with previous reports of ETS2 as a tumor suppressor in both prostate and lung cancer (27,28). Interestingly, HNSCC, where ETS2 has been described as an oncogene (19), had the lowest median levels of ZMYND11 of any tumor type analyzed (Supplementary Figure S5).

These data suggest that ZMYND11 is a tumor suppressor in prostate and non-small cell lung cancer. To further explore this hypothesis, we used TCGA data to test if higher or lower ZMYND11 expression was associated with recurrence free survival. In prostate adenocarcinoma, lower than median ZMYND11 expression trended toward lower recurrence free survival, but this result did not reach statistical significance ($P = 0.0971$, Figure 7D). In non-small cell lung cancers, tumors with low ZMYND11 expression had significantly lower recurrence free survival ($P = 0.00506$, Figure 7E). Together these data indicate a role for ZMYND11 to function in a tumor suppressive manner by allowing ETS2 to attenuate ETS1 function.

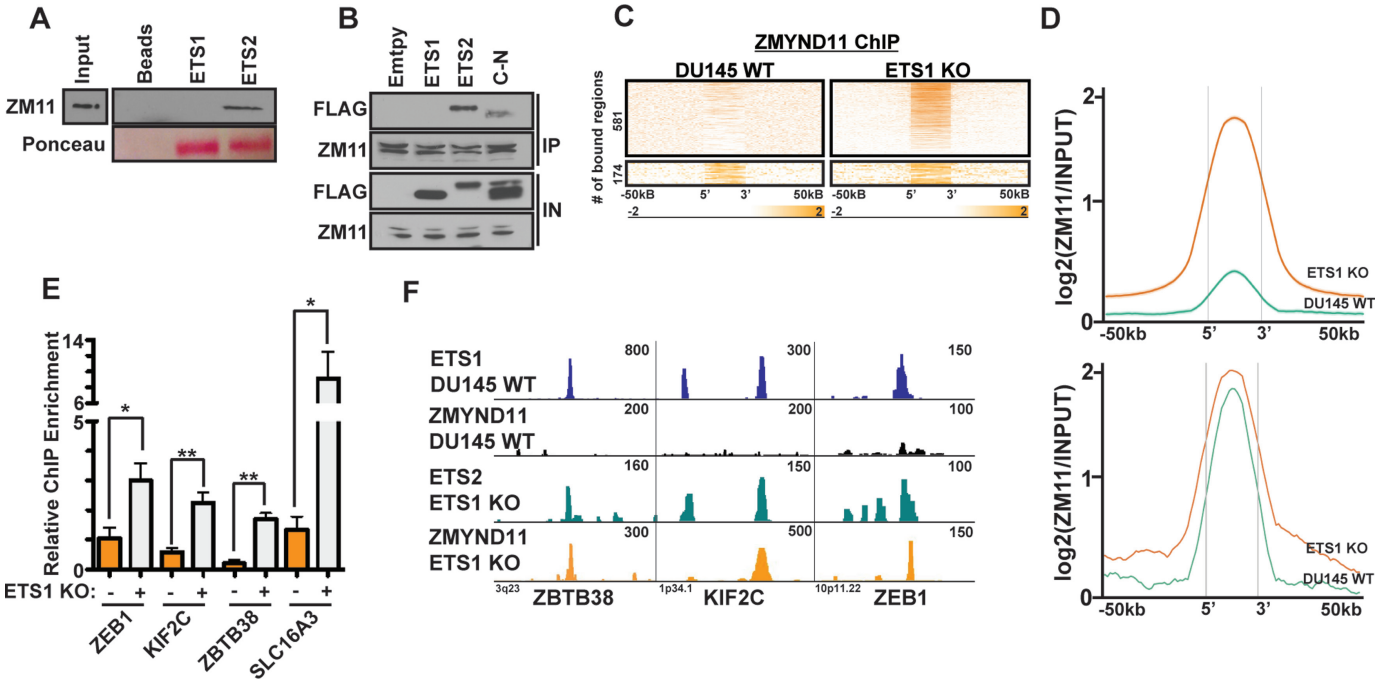

Figure 6. The co-repressor ZMYND11 specifically interacts with ETS2. (**A**) Anti-ZMYND11 (ZM11) immunoblot of proteins from PC3 nuclear extract that bind purified ETS1 or ETS2. Ponceau stain of same gel indicates amount of purified protein. (**B**) Extracts from DU145 cells expressing FLAG-ETS1, FLAG-ETS2 or FLAG-C-N were co-immunoprecipitated with ZMYND11 antibody and immunoblotted with anti-FLAG. (**C**) Heatmap of ChIP-seq enrichment for ZMYND11 within either 581 ETS1/2 co-bound regions, or 174 common ZMYND11 bound regions not bound by ETS1/2 in DU145 WT or DU145 ETS1 KO cell lines. Flanking regions extend ±50 kb, center region spans 500 bp. (**D**) Average ZMYND11 density profile of same regions from (C), with ETS1/2 bound regions on top and regions lacking ETS1/2 in lower panel. (**E**) ChIP-qPCR of ZMYND11 at known ETS1/2 co-bound regions in DU145 WT versus ETS1 KO cell lines. Data shown as mean and SEM of three biological replicates. All *P*-values (* < 0.05, ** < 0.01, *** < 0.001, n.s > 0.05) by *t*-test. (**F**) ChIP-seq enrichment of indicated factors across three ETS1/2 bound enhancers.

DISCUSSION

Here we report a specific mechanism that differentiates the two homologous ETS transcription factors, ETS1 and ETS2. Due to a specific protein-protein interaction between the N-terminus of ETS2 and the co-repressor ZMYND11, ETS1 and ETS2 had different transactivation potential, resulting in opposite regulation of gene expression when ETS1 and ETS2 compete for the same binding site. Mapping the ETS2 cistrome revealed that these factors do bind the same genomic regions, and gain of ZMYND11 binding at these regions in an ETS1 knockout line is consistent with binding site competition. However, at a fraction of ETS1/2 co-bound sites, ETS2 does appear to compete with ETS1 without ZMYND11 recruitment, perhaps suggesting a redundant role at these targets. Interestingly, ZMYND11 levels correlate with the ability of ETS2 to variably act as either an oncogene or tumor suppressor in epithelial cancers. Therefore, these finding suggest a specific mechanism that establishes an axis that tips the oncogenic function of the two highly homologous transcription factors, ETS1 and ETS2.

ETS2 can have distinct functions within different types of cancer cells. For example, ETS2 functions as an oncogene in some cancers, such as HNSCC (19), but a tumor suppressor in others, such as prostate (28) and intestine (26). Our characterization of a role for ZMYND11 in mediating transcriptional attenuation by ETS2, and the correlation of low ZMYND11 levels in cell types where ETS2 acts oncogenic, indicates a potential role for ZMYND11 expression in mediating these distinct functions. It will be interesting to determine if this role for ZMYND11 also regulates other ETS2 functions such as roles in tumor microenvironment. ETS2 expression in cancer associated fibroblasts and tumor-associated macrophages have been shown to correlate with poorer outcomes in breast cancers (42–44) and to promote the ability of colonic stem cells to aberrantly divide and colonize into tumors (25). These functions are often the opposite of the role of ETS2 in the tumor cells. These studies highlight the continued dichotomy in explaining ETS2 function, and the ZMYND11 interaction may only be one mechanism that determines how ETS2 will function in a tumor promoting or inhibiting manner.

Our analysis of TCGA data suggests that ZMYND11 is a tumor suppressor in prostate and lung cancer (Figure 7C and D). This is consistent with a previous report that ZMYND11 acts as a tumor suppressor in breast cancer (41). ZMYND11 acts in part, by recruitment of N-CoR and can repress the function of transcriptional activators, such as E1A, EBNA-2 and Myb (45,46). Endogenous co-immunoprecipitation experiments indicate that ETS2 also interacts with ZMYND11 (40), and our data suggest that the competition between the ETS2/ ZMYND11 complex and ETS1 provides a tumor suppressive function to ETS2. ETS1 and ETS2 are expressed in many malignancies from leukemias to carcinomas, therefore, ZMYND11 may func-

tion as a global tumor suppressor that may serve a diagnostic marker for outcomes in a wide variety of cancer types.

ZMYND11 is known to interact with transcription factors via an MYND domain, which binds a PXLXP motif present on the interacting factor (45). Interestingly, both ETS1 and ETS2 have a PXLXP motif in their N-terminus, however our data indicates that only the N-terminus of ETS2 can bind ZMYND11 indicating that binding can be influenced by other sequence differences. Both ETS1 and ETS2 are major downstream nuclear effectors of the RAS/ERK kinase cascade (9) and we demonstrate that both ETS1 and ETS2 bind at loci enriched in the RAS-responsive ETS/AP-1 cis-regulatory element (Figure 3B). The PXLXP motif on ETS2 (PLLTP) includes the ERK phosphorylation site T72. It has been reported that ERK phosphorylation of the T72 residue on ETS2 relieves the ZMYND11 interaction (40). It is interesting to speculate whether ZMYND11 binding might also inhibit phosphorylation of T72, leading to loss of RAS/ERK responsiveness.

Specific interacting partners that regulate the functions of ETS1 and ETS2 via the N-terminus, like ZMYND11, may also be responsible for other divergent functions such as differences in regulating gene expression leading to B cell activation into antibody-secreting cells (23). Further, the N-terminus of ETS1 and ETS2 appears to be a hotspot for evolutionary divergence of the two genes from a common ancestor. In chickens, an extended N-terminal ETS1 (p68) isoform is expressed, and the p68 ETS1 N-terminus has a similar function to the ETS2 N-terminus (47). Whether this function is related to ZMYND11 binding is unknown.

Recently it has been discovered that ZMYND11 functions as a reader of the Lysine 36 trimethylation (K36me3) mark on the histone variant H3.3 (41). The deposition of K36me3 occurs in the gene bodies, and subsequent recruitment of ZMYND11 to gene bodies leads to changes in transcriptional elongation and splicing (41,48). Interestingly, the most enriched KEGG pathway upregulated by ZMYND11 knockdown cells in a previous report (41) was 'Focal adhesion', which matches our pathway most enriched in genes bound specifically by ETS1 and ETS2 (Table 1). Therefore, it seems possible that ETS2 plays a key role in the recruitment of ZMYND11 to these tumor suppressor genes.

Taken together, our findings indicate a novel mechanism responsible for the divergent oncogenic phenotypes mediated by ETS1 and ETS2 in epithelial cancers and point the way for treatment options that could increase the function of ZMYND11 and ETS2 at the expense of ETS1.

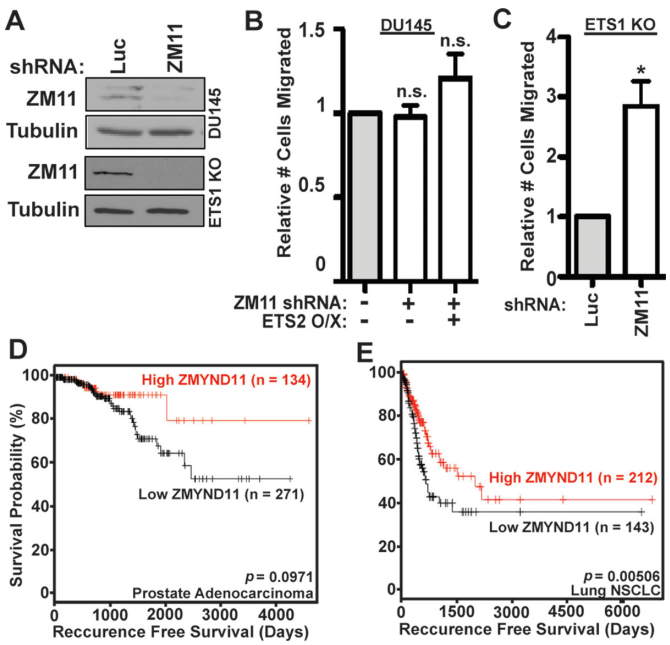

Figure 7. ZMYND11 is a putative tumor suppressor. (**A**) Immunoblot of DU145 or DU145 ETS1 knockout cells stably expressing ZMYND11 (ZM11) shRNA. Anti-tubulin blot is included as a loading control. (**B**) Transwell migration of DU145 cells expressing ZMYND11 shRNA and over-expression of ETS2 as indicated, shown as mean and SEM ($n = 3$). (**C**) Transwell migration of DU145 ETS1 knockout cells expressing ZMYND11 shRNA or luciferase (luc) shRNA control, shown as mean and SEM ($n = 3$). *P*-value (* < 0.05) by *t*-test. (**D**) Kaplan–Meier analysis of ZMYND11 high versus low RNA expression in TCGA prostate adenocarcinoma data. *P*-value calculated via Chi-square test with one degree of freedom. (**E**) Kaplan–Meier analysis as in (D) for non-small cell lung cancer.

ACCESSION NUMBER

GSE86240

SUPPLEMENTARY DATA

Supplementary Data are available at NAR Online.

ACKNOWLEDGEMENTS

The authors would like to thank Justin Budka for bioinformatic conversations and helpful analytic direction and the Indiana University Center for Genomics and Bioinformatics for next generation sequencing.

FUNDING

American Cancer Society Research Scholar Award [RSG-13-215-01-DMC]; Indiana University Vice Provost for Research through the Faculty Support Program; IU Simon Cancer Center P30 Support Grant [P30CA82709 to P.C.H.]; Medical Sciences Doane and Eunice Wright Memorial Fellowship (to J.P.P.). Funding for open access charge: Indiana University School of Medicine.
Conflict of interest statement. None declared.

REFERENCES

1. Downward,J. (2003) Targeting RAS signalling pathways in cancer therapy. *Nat. Rev. Cancer*, **3**, 11–22.
2. Yang,S.H., Sharrocks,A.D. and Whitmarsh,A.J. (2003) Transcriptional regulation by the MAP kinase signaling cascades. *Gene*, **320**, 3–21.
3. Campbell,P.M. and Der,C.J. (2004) Oncogenic Ras and its role in tumor cell invasion and metastasis. *Sem. Cancer Biol.*, **14**, 105–114.
4. Fafeur,V., Tulasne,D., Queva,C., Vercamer,C., Dimster,V., Mattot,V., Stehelin,D., Desbiens,X. and Vandenbunder,B. (1997) The ETS1 transcription factor is expressed during epithelial-mesenchymal transitions in the chick embryo and is activated in scatter factor-stimulated MDCK epithelial cells. *Cell Growth Differ.*, **8**, 655–665.

5. Fowles,L.F., Martin,M.L., Nelsen,L., Stacey,K.J., Redd,D., Clark,Y.M., Nagamine,Y., McMahon,M., Hume,D.A. and Ostrowski,M.C. (1998) Persistent activation of mitogen-activated protein kinases p42 and p44 and ets-2 phosphorylation in response to colony-stimulating factor 1/c-fms signaling. *Mol. Cell. Biol.*, **18**, 5148–5156.
6. Plotnik,J.P., Budka,J.A., Ferris,M.W. and Hollenhorst,P.C. (2014) ETS1 is a genome-wide effector of RAS/ERK signaling in epithelial cells. *Nucleic Acids Res.*, **42**, 11928–11940.
7. Hollenhorst,P.C., Jones,D.A. and Graves,B.J. (2004) Expression profiles frame the promoter specificity dilemma of the ETS family of transcription factors. *Nucleic Acids Res.*, **32**, 5693–5702.
8. Watson,D.K., McWilliams,M.J., Lapis,P., Lautenberger,J.A., Schweinfest,C.W. and Papas,T.S. (1988) Mammalian ets-1 and ets-2 genes encode highly conserved proteins. *Proc. Natl. Acad. Sci. U.S.A.*, **85**, 7862–7866.
9. Yang,B.S., Hauser,C.A., Henkel,G., Colman,M.S., Van Beveren,C., Stacey,K.J., Hume,D.A., Maki,R.A. and Ostrowski,M.C. (1996) Ras-mediated phosphorylation of a conserved threonine residue enhances the transactivation activities of c-Ets1 and c-Ets2. *Mol. Cell. Biol.*, **16**, 538–547.
10. Kopp,J.L., Wilder,P.J., Desler,M., Kim,J.H., Hou,J., Nowling,T. and Rizzino,A. (2004) Unique and selective effects of five Ets family members, Elf3, Ets1, Ets2, PEA3, and PU.1, on the promoter of the type II transforming growth factor-beta receptor gene. *J. Biol. Chem.*, **279**, 19407–19420.
11. Foulds,C.E., Nelson,M.L., Blaszczak,A.G. and Graves,B.J. (2004) Ras/mitogen-activated protein kinase signaling activates Ets-1 and Ets-2 by CBP/p300 recruitment. *Mol. Cell. Biol.*, **24**, 10954–10964.
12. Wei,G., Srinivasan,R., Cantemir-Stone,C.Z., Sharma,S.M., Santhanam,R., Weinstein,M., Muthusamy,N., Man,A.K., Oshima,R.G., Leone,G. *et al.* (2009) Ets1 and Ets2 are required for endothelial cell survival during embryonic angiogenesis. *Blood*, **114**, 1123–1130.
13. Kabbout,M., Dakhlallah,D., Sharma,S., Bronisz,A., Srinivasan,R., Piper,M., Marsh,C.B. and Ostrowski,M.C. (2014) MicroRNA 17-92 cluster mediates ETS1 and ETS2-dependent RAS-oncogenic transformation. *PLoS One*, **9**, e100693.
14. Wei,G.H., Badis,G., Berger,M.F., Kivioja,T., Palin,K., Enge,M., Bonke,M., Jolma,A., Varjosalo,M., Gehrke,A.R. *et al.* (2010) Genome-wide analysis of ETS-family DNA-binding in vitro and in vivo. *EMBO J.*, **29**, 2147–2160.
15. Bories,J.C., Willerford,D.M., Grevin,D., Davidson,L., Camus,A., Martin,P., Stehelin,D. and Alt,F.W. (1995) Increased T-cell apoptosis and terminal B-cell differentiation induced by inactivation of the Ets-1 proto-oncogene. *Nature*, **377**, 635–638.
16. Muthusamy,N., Barton,K. and Leiden,J.M. (1995) Defective activation and survival of T cells lacking the Ets-1 transcription factor. *Nature*, **377**, 639–642.
17. Man,A.K., Young,L.J., Tynan,J.A., Lesperance,J., Egeblad,M., Werb,Z., Hauser,C.A., Muller,W.J., Cardiff,R.D. and Oshima,R.G. (2003) Ets2-dependent stromal regulation of mouse mammary tumors. *Mol. Cell. Biol.*, **23**, 8614–8625.
18. Lamm,W., Vormittag,L., Turhani,D., Erovic,B.M., Czembirek,C., Eder-Czembirek,C. and Thurnher,D. (2005) The effect of nimesulide, a selective cyclooxygenase-2 inhibitor, on Ets-1 and Ets-2 expression in head and neck cancer cell lines. *Head Neck*, **27**, 1068–1072.
19. Yang,H., Schramek,D., Adam,R.C., Keyes,B.E., Wang,P., Zheng,D. and Fuchs,E. (2015) ETS family transcriptional regulators drive chromatin dynamics and malignancy in squamous cell carcinomas. *Elife*, **4**, e10870.
20. Smith,A., Teknos,T.N. and Pan,Q. (2013) Epithelial to mesenchymal transition in head and neck squamous cell carcinoma. *Oral. Oncol.*, **49**, 287–292.
21. Takai,N., Miyazaki,T., Nishida,M., Nasu,K. and Miyakawa,I. (2002) c-Ets1 is a promising marker in epithelial ovarian cancer. *Int. J. Mol. Med.*, **9**, 287–292.
22. Patton,S.E., Martin,M.L., Nelsen,L.L., Fang,X., Mills,G.B., Bast,R.C. Jr and Ostrowski,M.C. (1998) Activation of the ras-mitogen-activated protein kinase pathway and phosphorylation of ets-2 at position threonine 72 in human ovarian cancer cell lines. *Cancer Res.*, **58**, 2253–2259.
23. John,S., Russell,L., Chin,S.S., Luo,W., Oshima,R. and Garrett-Sinha,L.A. (2014) Transcription factor Ets1, but not the closely related factor Ets2, inhibits antibody-secreting cell differentiation. *Mol. Cell. Biol.*, **34**, 522–532.
24. Dittmer,J. (2003) The biology of the Ets1 proto-oncogene. *Mol. Cancer*, **2**, 29.
25. Munera,J., Cecena,G., Jedlicka,P., Wankell,M. and Oshima,R.G. (2011) Ets2 regulates colonic stem cells and sensitivity to tumorigenesis. *Stem Cells*, **29**, 430–439.
26. Sussan,T.E., Yang,A., Li,F., Ostrowski,M.C. and Reeves,R.H. (2008) Trisomy represses Apc(Min)-mediated tumours in mouse models of Down's syndrome. *Nature*, **451**, 73–75.
27. Kabbout,M., Garcia,M.M., Fujimoto,J., Liu,D.D., Woods,D., Chow,C.W., Mendoza,G., Momin,A.A., James,B.P., Solis,L. *et al.* (2013) ETS2 mediated tumor suppressive function and MET oncogene inhibition in human non-small cell lung cancer. *Clin. Cancer Res.*, **19**, 3383–3395.
28. Linn,D.E., Penney,K.L., Bronson,R.T., Mucci,L.A. and Li,Z. (2016) Deletion of interstitial genes between TMPRSS2 and ERG promotes prostate cancer progression. *Cancer Res.*, **76**, 1869–1881.
29. Stewart,S.A., Dykxhoorn,D.M., Palliser,D., Mizuno,H., Yu,E.Y., An,D.S., Sabatini,D.M., Chen,I.S., Hahn,W.C., Sharp,P.A. *et al.* (2003) Lentivirus-delivered stable gene silencing by RNAi in primary cells. *RNA*, **9**, 493–501.
30. Dull,T., Zufferey,R., Kelly,M., Mandel,R.J., Nguyen,M., Trono,D. and Naldini,L. (1998) A third-generation lentivirus vector with a conditional packaging system. *J. Virol.*, **72**, 8463–8471.
31. Selvaraj,N., Budka,J.A., Jerde,T.J., Ferris,M.W. and Hollenhorst,P.C. (2014) Prostate cancer ETS rearrangements switch a cell migration gene expression program from RAS/ERK to PI3K/AKT regulation. *Mol. Cancer*, **13**, 61.
32. Ran,F.A., Hsu,P.D., Wright,J., Agarwala,V., Scott,D.A. and Zhang,F. (2013) Genome engineering using the CRISPR-Cas9 system. *Nature Protocols*, **8**, 2281–2308.
33. Hollenhorst,P.C., Ferris,M.W., Hull,M.A., Chae,H., Kim,S. and Graves,B.J. (2011) Oncogenic ETS proteins mimic activated RAS/MAPK signaling in prostate cells. *Genes Dev.*, **25**, 2147–2157.
34. Selvaraj,N., Kedage,V. and Hollenhorst,P.C. (2015) Comparison of MAPK specificity across the ETS transcription factor family identifies a high-affinity ERK interaction required for ERG function in prostate cells. *Cell Commun. Signal.*, **13**, 1–14.
35. Kandoth,C., McLellan,M.D., Vandin,F., Ye,K., Niu,B., Lu,C., Xie,M., Zhang,Q., McMichael,J.F., Wyczalkowski,M.A. *et al.* (2013) Mutational landscape and significance across 12 major cancer types. *Nature*, **502**, 333–339.
36. Peinado,H., Olmeda,D. and Cano,A. (2007) Snail, Zeb and bHLH factors in tumour progression: an alliance against the epithelial phenotype? *Nat. Rev. Cancer*, **7**, 415–428.
37. Hollenhorst,P.C., Shah,A.A., Hopkins,C. and Graves,B.J. (2007) Genome-wide analyses reveal properties of redundant and specific promoter occupancy within the ETS gene family. *Genes Dev.*, **21**, 1882–1894.
38. Hollenhorst,P.C., Chandler,K.J., Poulsen,R.L., Johnson,W.E., Speck,N.A. and Graves,B.J. (2009) DNA specificity determinants associate with distinct transcription factor functions. *PLoS Gen.*, **5**, e1000778.
39. Gangwal,K., Sankar,S., Hollenhorst,P.C., Kinsey,M., Haroldsen,S.C., Shah,A.A., Boucher,K.M., Watkins,W.S., Jorde,L.B., Graves,B.J. *et al.* (2008) Microsatellites as EWS/FLI response elements in Ewing's sarcoma. *Proc. Natl. Acad. Sci. U.S.A.*, **105**, 10149–10154.
40. Wei,G., Schaffner,A.E., Baker,K.M., Mansky,K.C. and Ostrowski,M.C. (2003) Ets-2 interacts with co-repressor BS69 to repress target gene expression. *Anticancer Res.*, **23**, 2173–2178.
41. Wen,H., Li,Y., Xi,Y., Jiang,S., Stratton,S., Peng,D., Tanaka,K., Ren,Y., Xia,Z., Wu,J. *et al.* (2014) ZMYND11 links histone H3.3K36me3 to transcription elongation and tumour suppression. *Nature*, **508**, 263–268.
42. Wallace,J.A., Li,F., Balakrishnan,S., Cantemir-Stone,C.Z., Pecot,T., Martin,C., Kladney,R.D., Sharma,S.M., Trimboli,A.J., Fernandez,S.A. *et al.* (2013) Ets2 in tumor fibroblasts promotes angiogenesis in breast cancer. *PLoS One*, **8**, e71533.
43. Zabuawala,T., Taffany,D.A., Sharma,S.M., Merchant,A., Adair,B., Srinivasan,R., Rosol,T.J., Fernandez,S., Huang,K., Leone,G. *et al.* (2010) An ets2-driven transcriptional program in tumor-associated

macrophages promotes tumor metastasis. *Cancer Res.*, **70**, 1323–1333.
44. Tynan,J.A., Wen,F., Muller,W.J. and Oshima,R.G. (2005) Ets2-dependent microenvironmental support of mouse mammary tumors. *Oncogene*, **24**, 6870–6876.
45. Ansieau,S. and Leutz,A. (2002) The conserved Mynd domain of BS69 binds cellular and oncoviral proteins through a common PXLXP motif. *J. Biol. Chem.*, **277**, 4906–4910.
46. Masselink,H., Vastenhouw,N. and Bernards,R. (2001) B-myb rescues ras-induced premature senescence, which requires its transactivation domain. *Cancer Lett.*, **171**, 87–101.
47. Albagli,O., Soudant,N., Ferreira,E., Dhordain,P., Dewitte,F., Begue,A., Flourens,A., Stehelin,D. and Leprince,D. (1994) A model for gene evolution of the ets-1/ets-2 transcription factors based on structural and functional homologies. *Oncogene*, **9**, 3259–3271.
48. Guo,R., Zheng,L., Park,J.W., Lv,R., Chen,H., Jiao,F., Xu,W., Mu,S., Wen,H., Qiu,J. *et al.* (2014) BS69/ZMYND11 reads and connects histone H3.3 lysine 36 trimethylation-decorated chromatin to regulated pre-mRNA processing. *Mol. Cell*, **56**, 298–310.